ELSEVIER

Journal of Chromatography A, 738 (1996) 11–23

JOURNAL OF CHROMATOGRAPHY A

Optimization of indirect ultraviolet detection in high-performance liquid chromatography and capillary electrophoresis

F. Steiner, W. Beck, H. Engelhardt*

Universität des Saarlandes, Angewandte Physikalische Chemie, D-66123 Saarbrücken, Germany

First received 24 December 1993; revised manuscript received 9 January 1996; accepted 12 January 1996

Abstract

The similarities and differences in indirect UV detection in ion-exchange chromatography (IEC) and capillary zone electrophoresis (CZE) are discussed. In IEC the UV absorption of the buffer is the limiting factor, because of the relative long detection path length of usually 10 mm. The highest signal-to-noise ratios are obtained at low buffer concentrations. As the retention time is also determined by the buffer concentration, the exchange capacity of the stationary phase additionally has to be optimized. In practice, it is optimal to work close to the cut-off of the buffer solution to achieve the highest detection sensitivity. In CZE, the UV absorption of the buffer usually does not cause any problems because of the far shorter optical path length, which is determined by the inside diameter of the capillary. Here, the optimum detection sensitivity can be achieved when working at the absorption maximum of the buffer. Optimization of buffer concentration can follow the CZE requirements, i.e., low heat generation and low electrodispersion. Indirect UV detection in CZE gives surprisingly high detection sensitivity in the ppb range. The independence of signal-to-noise ratio of optical path length derived for IEC, when commonly used eluent concentrations and molar absorptivities are applied, is not valid for CZE. It is borderline case for optical path lengths above 4 mm. For a fast understanding of the influence of all variables in indirect UV detection, a simplified mathematical model was derived. This may be applied to both IEC and CZE measurements.

Keywords: Detection, LC; Detection, Electrophoresis; Inorganic anions; Metal cations

1. Introduction

The standard detection system in high-performance liquid chromatography (HPLC) and capillary zone electrophoresis (CZE) is the measurement of UV absorption at distinct wavelengths or the recording of spectra with a diode-array detector. Detection sensitivity is a function of the detection wavelength and the molar absorptivity of the solutes at these wavelengths. Solutes without suitable chromophores can only be detected if they can be derivatized either before or after the separation. However, this approach is not very convenient and may be the source of additional errors in quantitative and qualitative analysis.

Therefore, indirect detection techniques have been used in ion-pair chromatography (IPC) [1],

* Corresponding author.

0021-9673/96/$15.00
PII S0021-9673(96)00063-5

ion-exchange chromatography (IEC) [2–4] and (CZE) [5–8]. In all cases UV-absorbing components with similar properties as the solute to be analysed are added to the mobile phase or buffer. In the zones where the non-absorbing sample molecule migrates, the transparency of the mobile phase is better, and a negative signal (lower absorbance) is generated in the detector.

In addition to indirect UV detection, the principles of indirect detection modes have also been investigated for fluorescence and amperometric detection. An overview of the fundamentals and theories of charge displacement models and also volume displacement models in different indirect detection methods is given in Ref. [9].

Indirect detection techniques in IPC have not yet found wide application, owing to some intrinsic disadvantages [1,10]. Because the added absorbing ion is adsorbed on the stationary phase, the distortion of this adsorption equilibrium by the sample and/or the solvent introduced by the injection gives rise to so-called system peaks, which could appear, in the worst case, in that range of the chromatogram where the solutes to be analysed are eluted. Optimization of separation was not facilitated under these circumstances.

An additional disadvantage of indirect detection in IPC is that the peaks appeared either as positive deviations from the baseline, when eluted after the system peak, or as negative deviations in front of the system peak [1]. Quantification has been extremely difficult in these cases. The study of the types and elution order of system peaks gave some interesting insights into the adsorption equilibrium of mobile phase components with reversed-phase stationary phases [10,11].

The application of indirect UV detection is in principle much easier and more understandable in IEC [2,3]. The stoichiometric ion-exchange process requires for the displacement of the non-absorbing solutes a corresponding amount of UV-absorbing competing ions in the buffer. Because of the required electroneutrality in the buffer, the UV-absorbing ions displace a corresponding amount of charges of solute ions from the ion exchanger. In the buffer solution the transparency increases, as shown schematically in Fig. 1. Theoretically, it should be possible to calculate the signal size if the spectra of the eluting ions are known. From this, it can be deduced that the detection sensitivity must be identical for all non-absorbing ions of identical charge. Indirect UV detection in IEC also has not yet found wide application, because the sensitivity of the commonly used conductimetric detectors, especially in combination with suppression techniques, is a factor 10–100 better for anion detection. Also, good commercial instrumentation is available.

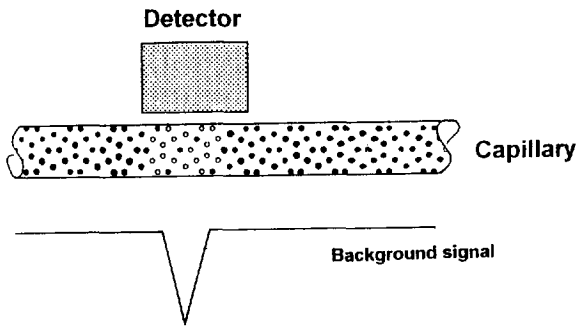

Fig. 1. Principle of indirect UV detection. ● = UV-absorbing buffer, ○ = solute without UV absorbance.

The application of indirect detection techniques in CZE has been described earlier [12,13], but the significance of this technique in CZE became obvious through the sensitive detection and high speed of analysis of anions [5] and cations [6,14]. Despite the short path length in CZE (average capillary diameter), surprisingly low detection limits could be achieved. Some theories have been proposed to try to explain this fact [15].

With liquid chromatographic UV detectors, the light path length is well defined and reaches typical values from 4 to 10 mm. The relatively high absorption of the eluent in indirect UV detection causes increased noise of the detector baseline. Small changes in the high background signal, caused by the elution of the UV-transparent sample solutes, limit the detection sensitivity. The dependence of the signal-to-noise ratio on the concentration of the absorbing ion in the

eluent has been discussed [2]; however, there is no knowledge of whether it is possible to improve the signal-to-noise ratio at a constant path length by changing the detection wavelength. A reduction of the background absorbance by shortening the light path in the detector requires a lot of technical effort, and such detectors are hardly commercially available.

In CZE, in contrast, the path length can be varied by changing the capillary diameter. A complete knowledge of the dependence of signal-to-noise ratio on the capillary diameter is of great importance for optimizing the efficiency and speed of analysis in CZE by variation of the capillaries.

The signal generation discussed in IEC cannot easily be transferred without changes to CZE, because there is no stationary phase present. In CZE, the charge displacement mechanism is totally different from that in IEC. The aim of this paper is therefore to discuss the fundamentals of signal generation and the sources of noise in CZE in comparison with IEC, to optimize the signal-to-noise ratio and hence the detection sensitivity for CZE and IEC applications using indirect UV detection.

A simplified theory, neglecting the influences of an individual displacement ratio for the charges, will be described which is valid within a certain range in both CZE and IEC and permits fundamental predictions, to help inexperienced users understanding the various parameters for optimization.

2. Fundamentals of indirect UV detection

The simplified mechanism of charge displacement for IEC is far better understood than for CZE. Therefore, the fundamentals of the method in the case of chromatography will be described first and then transferred to CZE afterwards.

The concentration of the UV-absorbing eluent component should be so small that the Lambert–Beer law is still valid. This is the only assumption made. The addition of the absorbing eluent component give rise to an extinction E_1, commonly called the background signal, which is set to zero ($E_1 = 0$) before the separation begins. In IEC the displacement of the UV-absorbing eluent components [with molar absorptivity extinction coefficient, ε_b] by an equal amount of transparent solute ions reduces the background signal for an extinction value E_3. This change in the extinction is, in the ideal case, the measured signal in indirect UV detection. However , this value is reduced for an extinction E_2 when the solute ions have a certain absorptivity (molar absorptivity ε_s) at the detection wavelength. As can be seen schematically in Fig. 2, the signal is hence dependent on the values of E_2 and E_3. The buffer concentration c_b giving rise to the extinction E_1 is the dynamic reserve of the eluent and may never be exceeded by the sample concentration c_s without extreme overloading of the system. No higher signal than $-E_1$ can occur.

Extinction of the buffer: $E_1 = \varepsilon_b c_b d$ (1)

Extinction of the solute: $E_2 = \varepsilon_s c_s d$ (2)

Reduction of extinction by displacement:

$$E_3 = \varepsilon_b c_s d \quad (3)$$

For displacement, singly charged solute and buffer ions with concentrations c_s and c_b are considered. Here the optical path length is d. The signal at the peak maximum can be calculated [2]:

$$S = E_2 - E_3 = \varepsilon_s c_s d - \varepsilon_b c_s d \quad (4)$$

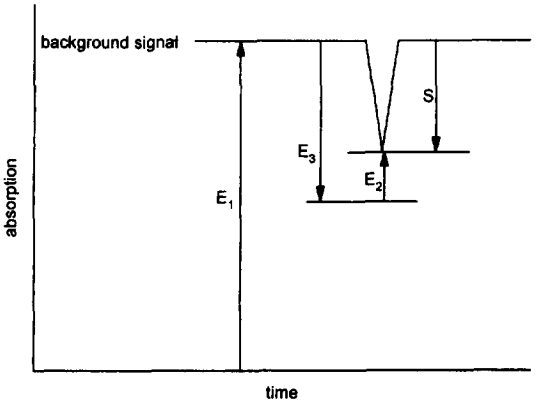

Fig. 2. Generation of the signal in indirect UV detection. For description, see text.

$$S = (\varepsilon_s - \varepsilon_b)c_s d \quad (5)$$

The dynamic reserve E_1 cannot be considered mathematically. If multivalent buffer and solute ions have to be considered, E_3 has to be corrected. With buffer ions carrying a charge z that are displaced by solute ions with charge x (assuming a 1:1 charge displacement), the extinction change E_3 can be described by

$$E_3 = \frac{x}{z} \cdot c_s \varepsilon_b d \quad (6)$$

Inserting this in Eq. 4, it follows for a signal with polyvalent ions that

$$S = \left(\varepsilon_s - \frac{x}{z} \cdot \varepsilon_b\right)c_s d = \varepsilon_b\left(\frac{\varepsilon_s}{\varepsilon_b} - \frac{x}{z}\right)c_s d \quad (7)$$

Eqs. 5 and 7 show the appearance of negative signals for the analysis of transparent ions ($\varepsilon_s = 0$). It can also be seen that for ions with an absorption at the working wavelength, positive peaks can also be expected for the case when $\varepsilon_s/\varepsilon_b > x/z$. Furthermore, if $\varepsilon_s/\varepsilon_b = x/z$, no signal can be observed. In this case, the detection wavelength has to be changed to be able to detect a peak. The larger the difference between ε_s and ε_b, the higher the detection sensitivity will be. Optimization strategies will be demonstrated by applying a diode-array detector. Of course, in Eqs. 5 and 7 an individual detector constant a has to be added if different detectors have to compared.

According to Small and Miller [2], the noise can be calculated by

$$N = nc_b \varepsilon_b d \quad (8)$$

If this equation holds, the signal-to-noise ratio should then be independent of the path length d of the detector as shown by the equation

$$\frac{S}{N} = \frac{a}{n} \cdot \frac{c_s\left(\varepsilon_s - \frac{x}{z} \cdot \varepsilon_b\right)}{c_b \varepsilon_b} \quad (9)$$

The validity of Eq. 9 has been proved in IEC for certain cases [2]. If this could be transferred to CZE, indirect UV detection would be very advantageous there, because the reduction of the path length (= capillary diameter) would permit the use of higher voltages (much easier heat dissipation), resulting in faster analysis without a loss in detection sensitivity.

Small and Miller's simplified theory [2] ignores other sources of noise besides the noise caused by the visualizing reagent in the system. On the other hand, it is feasible that in CZE, where one usually works close to the detection limit, noise originating in the detector optics, electronics and light sources may contribute to the overall detection noise. This has to be considered in Eq. 8 by an additional increment n_D. Hence the total noise N_{tot} may be calculated by

$$N_{tot} = nc_b \varepsilon_b d + n_D \quad (10)$$

To be able to transfer Small and Miller's theory of signal generation to CZE, one has to consider that the net charge of the ions in solution may not correspond to their formal charges and that they also differ in their mobilities. The influence of the mobilities has been predicted by the Kohlrausch regulation function [15]. This effect has been considered by introducing a displacement ratio factor R [16]. The displacement ratio R may be calculated with some mathematical effort [17–19], but these calculations are beyond the scope of this paper. The signal for indirect UV detection in CZE can thus be calculated by

$$S = a\left(\varepsilon_s - R \cdot \frac{x}{z} \cdot \varepsilon_b\right)c_s d \quad (11)$$

This leads to a modified equation for calculating the signal-to-noise ratio (S/N) in CZE:

$$\frac{S}{N} = \frac{a\left(\varepsilon_s - R \cdot \frac{x}{z} \cdot \varepsilon_b\right)c_s d}{nc_b \varepsilon_b d + n_D} = \frac{a\left(\frac{\varepsilon_s}{\varepsilon_b} - R \cdot \frac{x}{z}\right)c_s}{nc_b + \frac{n_D}{\varepsilon_b d}} \quad (12)$$

Refining the theory for IEC, a displacement ratio R might also be considered, e.g. to correct the deviations of the effective charge of the ions from the formal charge. Further, it should be also reasonable to consider an influence of the basic noise n_D from the HPLC detectors in indirect detection modes. Consequently, Eq. 12 should be valid in both HPLC and CZE. The validity of this theory will be tested by experiments in IEC and CZE.

3. Experimental

For HPLC measurements, the apparatus was composed of a Bischoff (Leonberg Germany), Model 2200 HPLC pump, a Rheodyne Model 7125 injection port (20-μl loop) and a Waters Model 990 photodiode-array detector with Waters 990 software on an NEC APC-IV personal computer (Waters Division of Millipore, Eschborn, Germany). The column (250 × 4.1 mm I.D.) was packed with a strong anion exchanger (triethylammoniummethylstyrene polymerized on 10-μm silica [20]).

The CZE measurements were performed with the following instruments and their data acquisition systems: Quanta 4000 from Millipore–Waters (Eschborn, Germany) with Maxima 825 software and an NEC Power Mate IV with A/D interface; P/ACE 2100 from Beckman (Munich, Germany) with P/ACE 2.01 software and an IBM 386 computer; and an HP^{3D}CE system from Hewlett-Packard (Waldbronn, Germany). A laboratory-made system [21] with a GAT PHD 601 multi-wavelength detector from GAT (Bremen, Germany) (identical with a Linear UV VIS 206) and a power supply HCN 35-35000 (FUG, Rosenheim, Germany) was also used.

CZE capillaries with I.D. between 25 and 160 μm (O.D. 370 μm) were purchased from Poly-Micro Technologies (Phoenix, AZ, USA). For all measurements Milli-Q water (Millipore, Eschborn, Germany) and buffer components from Fluka (Neu Ulm, Germany) were used. Imidazole was obtained from Merck (Darmstadt, Germany).

4. Results and discussion

4.1. IEC measurements

The theory of indirect UV detection permits the calculation of the signal size in the cases when the molar absorptivity of the buffer and solute ions are known. To prove the validity of the theory, an IEC separation of chloride, nitrite, bromide, nitrate and sulfate was performed. Iodide was added to this mixture, because this ion has an absorption maximum at 228 nm. For elution a 0.5 mM solution of phthalic acid was used (pH of the buffer = 6.5). The molar absorptivities of phthalate and the solutes were measured with the diode-array detector over the wavelength range 200–290 nm. The solute concentration c_p at the peak maximum was calculated with the equation [22].

$$c_p = \frac{m\sqrt{N}}{\sqrt{2\pi}V_m(1+k')} \tag{13}$$

where m is the amount of sample injected, N is the plate number of the solute peak with the capacity factor k' and V_m is the amount of eluent within the column (the total porosity ε_T of the stationary phase was 0.74).

In Table 1, the calculated (assuming a displacement ratio $R = 1$ and an effective charge of 2 for phthalate) and measured values of peak heights for the different solutes at various wavelengths are compared. One can see that the assumed displacement ratio of 1 is not observed. The ratios of measured to calculated signals are given as R^*. All measured values are higher (10–100%) than the calculated values. Only for the most strongly retained solute (sulfate) are the calculated peak heights higher. If one neglects the values at 240 and 280 nm, where the signals are certainly strongly affected by noise, the values for R^* are almost constant for a specific ion. In the case of iodide the value at 250 nm should be neglected for the same reasons, because the measured signal is very small there. The deviations of R^* from unity can be explained by an additional, e.g., hydrophobic, retention mechanism. Also, the effective charge may differ in solution from the assumed values. Further sources of error and reasons for deviations between theory and practice might be differences between real and assumed peak shape and errors in recording the spectra of buffer and analyte ions with the HPLC diode-array detector.

In contrast to all other sample ions investigated, iodide shows an absorption within the applied wavelength range. Its absorption is at wavelengths below 250 nm higher than half the

Table 1
Comparison between measured and calculated peak heights in IEC and displacement ratios R^* calculated from proportion between measured and calculated value

Detection		Wavelength									
Ion	Signal	240 nm		250 nm		255 nm		265 nm		280 nm	
Chloride	Measured	−88.29	R^* = 1.38	−50.60	R^* = 1.55	−34.04	R = 1.59	−18.20	R^* = 1.48	−15.52	R^* = 1.38
	Calculated	−63.80		−32.63		−21.39		−12.33		−11.24	
Nitrite	Measured	−49.10	R* = 1.60	−34.22	R^* = 1.82	−24.21	R^* = 1.89	−13.06	R^* = 1.71	−11.30	R^* = 1.62
	Calculated	−30.60		−18.81		−12.83		−7.65		−6.98	
Bromide	Measured	−31.63	R^* = 1.59	−19.83	R^* = 1.95	−13.51	R^* = 2.03	−7.22	R^* = 1.88	−6.29	R^* = 1.80
	Calculated	−19.80		−10.13		−6.64		−3.83		−3.49	
Nitrate	Measured	−33.99	R^* = 1.10	−22.70	R^* = 1.36	−15.09	R^* = 1.36	−8.15	R^* = 1.27	−6.99	R^* = 1.20
	Calculated	−30.75		−16.73		−11.06		−6.38		−5.81	
Iodide	Measured	+10.90	R^* = 1.26	0.00	R^* = 0.89	−1.93	R^* = 1.16	−1.80	R^* = 1.18	−1.70	R^* = 1.15
	Calculated	+13.20		−0.50		−1.45		−1.50		−1.47	
Sulfate	Measured	−7.23	R^* = 0.55	−5.05	R^* = 0.75	−3.45	R^* = 0.78	−1.86	R^* = 0.73	−1.67	R^* = 0.72
	Calculated	−13.20		−6.75		−4.43		−2.55		−2.33	

For conditions, see text. Peak heights are given in mAU. Peak direction: − for negative peak, + for positive peak.

absorption (charge displacement 2 to 1) of the phthalate ion. Consequently, positive peaks are observed. As can be seen in Table 1 and Fig. 3, also in this case a good correspondence between calculated and measured peak heights can be observed. In the wavelength range between 250 and 290 nm, iodide can be detected by indirect UV detection (negative peaks). At a wavelength of 250 nm the absorption of iodide and phthalate balance each other. Consequently, no iodide peak can be detected at this wavelength. Of course, at wavelengths below 250 nm iodide determines the absorption and the peaks are going in the other direction.

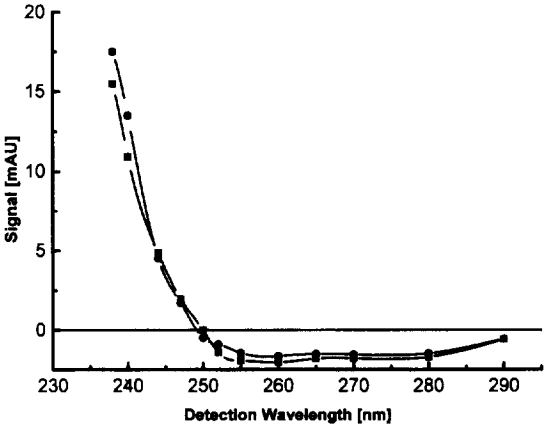

Fig. 3. Comparison of (■) measured and (●) calculated signals as a function of detection wavelength. Conditions: sample, iodide ion; buffer, 0.5 mM phthalate (pH 6.5); detector, Waters Model 990.

4.2. Influence of the eluent on the baseline noise

Optimization of IEC separations can be achieved by variations of the concentration of the buffer ion. An increase in this concentration always reduces retention. This optimization strategy has some limitations in indirect UV detection, because baseline noise is a direct function of the buffer absorption (Eq. 8). The path length d is given by the chromatographic equipment, and therefore the only possibility of reducing baseline noise is to change the detection wavelength to reduce the eluent absorption. Fig. 4 shows the dependence of the baseline noise on detection wavelength for three different buffer concentrations. For the two most convenient buffer concentrations (2.0 and 1.0 mM), the baseline noise is almost constant at lower levels down to a wavelength of 260 nm. With the more dilute buffer it is possible to work at wavelengths down to 250 nm. The noise can be directly correlated to the absorption of the buffer. As

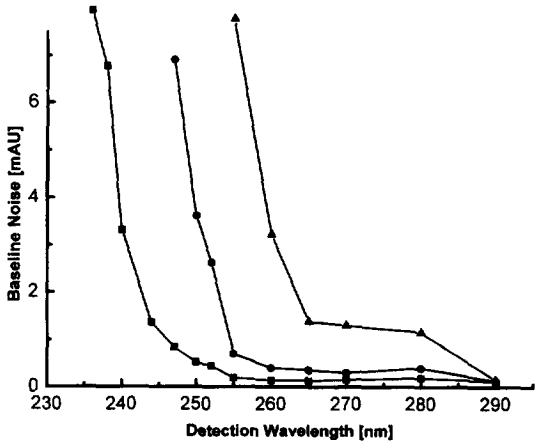

Fig. 4. Dependence of baseline noise on the detection wavelength. Conditions: buffer, (■) 0.5, (●) 1.0 and (▲) 2.0 m*M* phthalate; other conditions as in Fig. 3.

long as the Lambert–Beer law is valid (below an extinction of about 1.5 absorbance units), the baseline noise shows only a slight dependence on eluent absorption. Beyond these values the noise increases tremendously. For the detector used in this study, the baseline noise showed only a slight increase on going to higher buffer absorbance (lower wavelength), provided that the extinction did not exceed a value of 1.2 absorption units, which is within the validity of the Lambert–Beer law.

4.3. Detection limits

Detection limits are determined by the signal-to-noise ratio. The detection limit is usually defined for a signal-to-noise ratio of 3:1. To study the detection sensitivity achievable in IEC, the signal-to-noise ratio for the chloride peak was studied at different buffer concentrations as a function of the detection wavelength. Chloride was selected because it has no absorption and, as an early-eluting peak, its peak width and plate number were hardly affected by changes in the buffer concentration. At the highest buffer concentration used (2 m*M*), the signal height was a factor of two larger than with the more dilute buffers. This is due to the higher concentrations at the peak maximum when the k values are low. However, as the noise increases with this buffer at wavelengths below 265 nm (see Fig. 4), this peak-sharpening effect could not be used for improving the detection sensitivities. As can be seen in Fig. 5, the signal-to-noise ratio is a distinct function of the buffer concentration and the detection wavelength. The signal increases with increasing absorptivity of the eluent. At a wavelength of 290 nm the absorption of the phthalate ion is small. As the absorption maximum of the phthalate is approached, the detection sensitivity improves. At lower wavelength the noise increases (compare Fig. 4), and therefore the signal-to-noise ratio decreases. Similar signal-to-noise ratios have been obtained for the other ions.

For discussing the plots in Fig. 5, Eqs. 9 and 12 are slightly modified to be valid only for the case of a non-absorbing sample ion ($\varepsilon_s = 0$):
from Eq. 9:

$$\frac{S}{N} = \frac{-ac_s \cdot \frac{x}{z}}{nc_b} \tag{14}$$

from Eq. 12:

$$\frac{S}{N} = \frac{-aR \cdot \frac{x}{z} \cdot c_s}{nc_b + \frac{n_D}{\varepsilon_b d}} \tag{15}$$

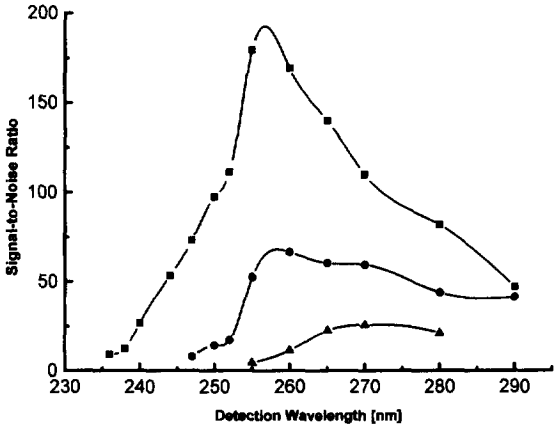

Fig. 5. Dependence of signal-to-noise ratio in IEC on the wavelength. Sample, chloride ion; other conditions as in Fig. 4.

With Eq. 14 it is not possible to describe the shapes of the plots in Fig. 5, because it is assumed that n is constant and ε_b does not appear in the equation. In Fig. 4 it has been shown that the noise increases exponentially close to the cut-off of the buffer solution. In this range n depends strongly on the buffer absorption. This explains the decrease in the signal-to-noise ratios at wavelengths beyond the cut-off. However, this also does not explain the improvement in the signal-to-noise ratio with increasing absorptivity of the buffer, especially at low buffer concentrations c_b.

From Eq. 15, it can be deduced that the basic (electronic, etc.) noise n_D of the detector cannot be neglected when a short optical path length d and/or a low buffer absorption ε_b are applied (small values for the product $\varepsilon_b d$). The influence of the basic noise n_D becomes even more important when low buffer concentrations are used. The assumptions in Small and Miller's simplified theory are only valid when the electronic noise of the detector is negligible and the optical path length and the buffer concentration and its absorptivity exceed a certain value.

The highest signal-to-noise ratios are obtained with low buffer concentrations. However, the chromatographic process requires a compromise. With low buffer concentrations the retention times are long and, hence, the concentration at the peak maximum becomes smaller owing to the chromatographic process. In IEC the exchange capacity of the stationary phase has to be optimized additionally in this way so that already with low buffer concentrations short analysis times are achieved. As in every chromatographic process, the retention is a function of the absorption capacity of the stationary phase and the elution strength of the eluent. For indirect detection in IEC, a counterbalance of capacity and elution strength is crucial for obtaining a high detection sensitivity.

When considering the influence of the detection wavelength, it is advantageous to detect close to the cut-off of the eluent. As long as the noise coefficient n remains constant, S/N increases with increasing ε_b.

4.4. Capillary electrophoresis

In IEC the signal in indirect UV detection originates from the displacement of the non-absorbing sample ions by absorbing buffer ions from the stationary phase and the resulting decrease in concentration of these buffer ions in the effluent. From the required electroneutrality in the presence of a constant counterion concentration, a stoichiometric displacement can be assumed. However, in CZE the relationships are not as simple, because no ion-exchange equilibrium exists. The displacement of ions in the background electrolyte is based on the Kohlrausch regulation function (KRF) [15].

The exact calculation of the displacement ratio between sample ions and buffer ions requires a considerable mathematical effort. Every ion in the buffer system, including the counterions, has to be taken into account. This problem may be solved by treatment as a linear eigenvalue problem, starting from coupled transport equations, as described for both HPLC and CZE [19].

A simple treatment similar to that applied in IEC is difficult, because no Gaussian peaks are observed. Hence the concentration at the peak maximum can only be calculated by assuming triangular peaks and applying Euclid geometry, that is to say that the maximum height is twice the averaged height of the triangle. The area proportional to the amount injected is hence the area of the rectangle described by the peak width times the average peak height. The concentration c_{max} at the peak maximum can be calculated by

$$c_{max} = \frac{2m_{inj}t_{mig}}{w_t L_{eff} r^2 \pi} \tag{16}$$

where w_t is in time units and r is the capillary radius. For the calculation of the displacement ratio R the signal measured has to be divided by the signal calculated by applying Eqs. 16 and 11 and inserting the detector constant a from Table 3 and ε_{214}(imidazole) = 5000 mol^{-1} cm^{-1}. The calculated displacement ratios are summarized in Table 2. Despite the rough approximation adopted, the simple approach permits the calcu-

Table 2
Calculated displacement ratios

Ion	t_{mig} (s)	w_t (s)	m_{inj} (pg)	c_{max} (mmol l^{-1})	S_{exp} (mAU)	S_{meas} (mAU)	R
K^+	125.06	3.4	40.4	0.034	1.61	3.91	3.05
Na^+	160.25	1.6	40.4	0.159	5.98	5.87	0.97
Ba^{2+}	169.23	1.4	40.4	0.032	2.41	3.47	1.45
Ca^{2+}	172.77	1.8	40.4	0.088	6.56	5.80	0.88
Mg^{2+}	179.86	2.6	40.4	0.104	7.83	7.48	0.94
Li^+	187.80	2.7	20.2	0.183	6.88	6.78	0.97

For the CZE cation separation a capillary of I.D. 75 μ and effective length 50 cm was applied.

lation of the expected signals in CZE. The interpretation of the deviations of R from unity is rather difficult and beyond the scope of this paper.

4.5. Signal-to-noise ratio and capillary diameter

As a consequence, the basic principles of displacement in indirect UV detection are valid also in CZE. Because of the small optical path length in CE (capillary diameter), it would be advantageous if S/N were to be independent of it. This would help to exploit fully the advantages of narrow capillaries in CZE (high voltages, short analysis times). Therefore, indirect UV detection was studied with capillaries with I.D. between 25 and 160 μm. Even when applying relatively high buffer concentrations and measuring close to the extinction maximum, the findings predicted by Small and Miller's [2] simplified equation could not be verified in CZE. As can be seen in Fig. 6, the detection noise increased linearly with increasing I.D. starting from a considerable intercept n_D (Eq. 10). For a more correct calculation of S/N in CZE, Eq. 12 has to be used. Consequently, S/N is not independent of the optical path length (capillary diameter).

Three different CE detectors were compared by measuring the influence of the capillary I.D. on S/N. For this comparison the individual detector constants a, n and n_D from Eq. 12 had to be determined. For the determination of a, the capillary was filled with water, the detector was set to zero and a 2 mM imidazole solution was introduced hydrodynamically. By assuming that the optical path length corresponds to the I.D. of the capillary and a molar absorptivity of 5000 mol^{-1} cm^{-1} for imidazole at 214 nm, the measured absorption was related to that calculated by Beer's law. These values for a are summarized in Table 3. From the slopes and intercepts in Fig. 6, as an example for one detector, the different noise parameters n and n_D of all three detectors could be calculated and are also included in Table 3. The values of n_D (detector noise) are in good agreement with the manufacturer's specification. It should be mentioned that all these measurements were achieved without

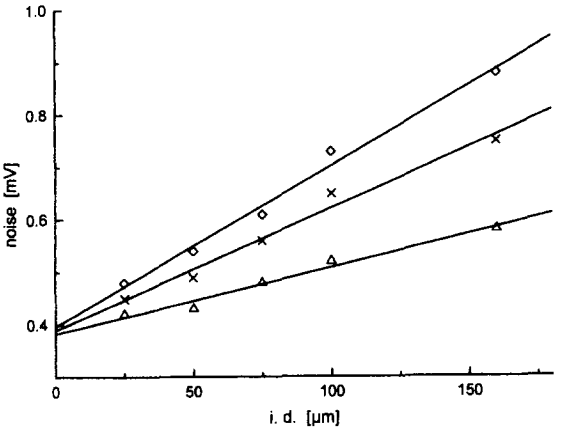

Fig. 6. Dependence of noise on the I.D. of capillaries for three different buffer concentrations. Conditions: Millipore/Waters Quanta 4000; buffer, imidazole–sulfuric acid (pH 4.6) (△) 25, (×) 50 and (◇) 75 mM; capillary, 40 cm × 25–160 μm I.D., 360 μm O.D. detection, indirect at 214 nm.

Table 3
Detector constants for different CZE equipment

Detector	a	n	n_D
Beckman P/ACE 2100	$0.497 \cdot \frac{AU_{measured}}{AU_{calculated}}$	$27 \cdot 10^{-6}$	$100\ AU \cdot 10^{-6}$
Millipore–Waters Quanta 4000	$0.317 \cdot \frac{V}{AU_{calculated}}$	$8.3 \cdot 10^{-6}$	$40\ V \cdot 10^{-6}$
GAT fast-scanning detector	$0.096 \cdot \frac{AU_{measured}}{AU_{calculated}}$	$5.5 \cdot 10^{-6}$	$10\ AU \cdot 10^{-6}$

a was determined from the height of a signal of a 2 mM solution of imidazole and n and n_D were determined from plots as shown for the Quanta 4000 in Fig. 6.

applying an electric field. In practice, the noise values (mainly n) will always be larger owing to convection and heat dissipation.

By inserting the experimentally determined values from Table 3 into Eq. 11, it is possible to calculate the S/N value as a function of capillary I.D.. These curves are depicted in Fig. 7. In these calculations a linear increase of noise with increase in capillary I.D. (Fig. 6) and validity of the Lambert–Beer law have been assumed. As can be seen in Fig. 7, S/N increases with increase in path length and above 4 mm it is almost independent of the path length. Small and Miller's simplified assumption is therefore only valid for LC measurements when the path length of the detectors is longer than 4 mm and the other assumptions discussed above are fulfilled. As can be seen from Eq. 12, the term n_D can be neglected when d becomes larger, provided that c_b and ε_b are not too small. The displacement of 1 mM imidazole by the equivalent amount of monovalent cations is assumed for fundamental calculations.

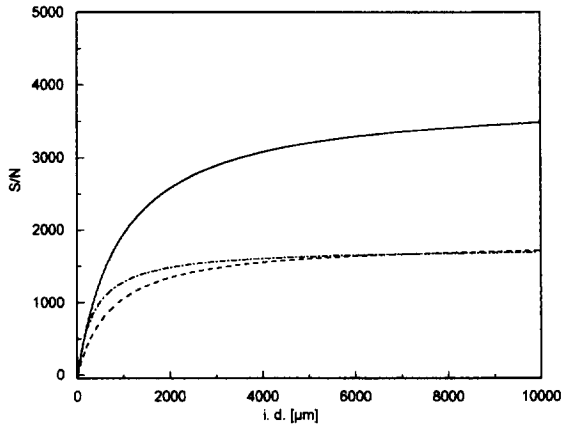

Fig. 7. Calculated signal-to-noise ratios and I.D. of the capillary. For calculations Eq. 12 was used with the values from Table 3 and $\varepsilon = 5000\ l\ mol^{-1}\ cm^{-1}$; 10 m$M$ imidazole; 1 mM displaced imidazole, displacement ratio $R = 1$; detectors from (– – –) Beckman P/ACE 2100, (——) Waters Quanta 4000 and (– · – · –) GAT PHD 601.

4.6. Detection limit

The ion-displacing mechanism permits the calculation of the detection limit if the detector and system constants have been measured. This is demonstrated in Fig. 8 for three different detectors and monovalent ion displacement. The slopes of the curves are a measure of the detection sensitivity. The S/N gives the detection limit. For the lithium ion a detection limit of 10 μmol l^{-1} was calculated, which corresponded well with the experimentally determined value of 7 μmol l^{-1} with the Waters instrument and the imidazole buffer system [6].

4.7. Signal-to-noise ratio as a function of detection wavelength

Diode-array detectors are becoming more and more available for CZE. They permit not only measurements of spectral data, but also the rapid optimization of S/N in indirect UV-detection. In

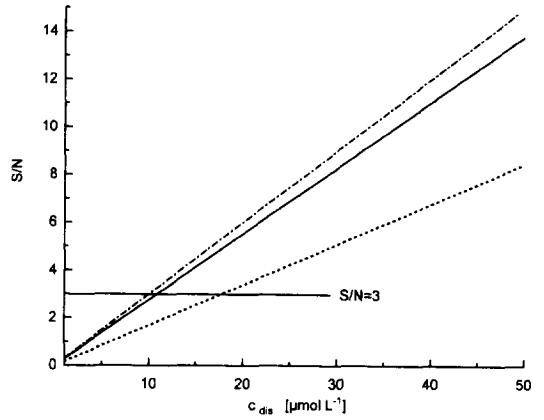

Fig. 8. Determination of the theoretical detection limit. For calculations Eq. 12 was used with the following parameters: $\varepsilon = 5000$ l mol^{-1} cm^{-1}; 10 m*M* imidazole; 75 μm I.D. capillary; displacement ratio $R = 1$; detector from (– – –) Beckman P/ACE 2100, (——) Waters Quanta 4000 and (– · – · –) GAT PHD 601.

Fig. 9 the dependence of the signal and the noise for an imidazole buffer as a function of detection wavelength is shown. Both curves have similar shapes corresponding to the predictions by Eqs. 10 and 11. As far as the investigated system is concerned, *S*/*N* shows a maximum at the absorption maximum of the background electrolyte, as demonstrated in Fig. 10. Here the lowest detection limits can be achieved by working at the absorption maximum of the background electrolyte. In LC, as discussed above, in almost all cases it is not possible to work at the absorption maxima, because with the larger optical path length there, the validity of the Lambert–Beer law is easily exceeded. In CZE, there is also a limitation of buffer concentration, because of secondary effects; e.g., higher Joule heat generation at higher buffer concentrations the noise increases, and at lower buffer concentration the concentration differences between sample plug and background electrolyte are the reason for asymmetric peaks (electrodispersion). Therefore, an optimum buffer concentration has to be selected, which depends on the I.D. of the capillary. For the most commonly used capillaries of 75 μm I.D., the optimum buffer concentration for indirect UV detection is in the range 5–8 m*M*.

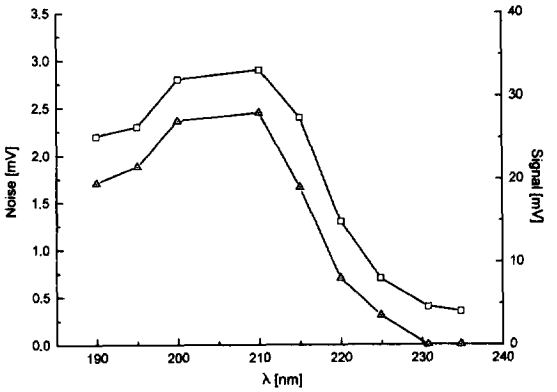

Fig. 9. Dependence of (△) the signal and (□) the noise on the detection wavelength. Conditions: Hewlett-Packard HP ^{3D}CE instrument; buffer, 10 m*M* imidazole–acetic acid (pH 4.9); capillary 61 cm × 75 μm I.D., 360 μ I.D., without bubble; detection, indirect, bandwidth 4 nm; ref., 450 with 80 nm bandwidth; injection, 5 kV for 5 s; field, 492 V cm^{-1}; sample, 0.5 m*M* potassium, sodium and lithium.

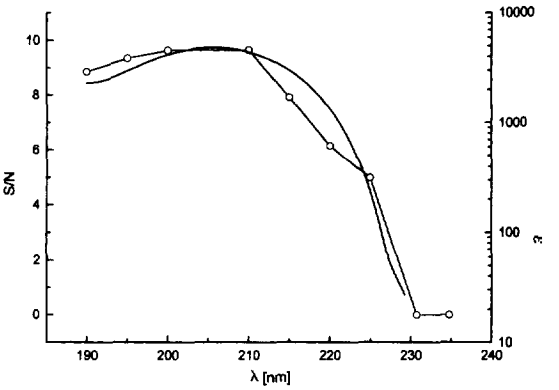

Fig. 10. Dependence of the signal-to-noise ratio (○) on the detection wavelength. Conditions as in Fig. 9; molar absorptivity (——) and spectral data from Ref. [23].

5. Conclusions

The basic rules for signal and noise generation in indirect UV detection are valid in IEC and CZE. As a first approximation, one can assume that equivalent charges of the eluting buffer or of the background electrolyte are displaced by the sample ions. The height of the signal in IEC and CZE is proportional to the relationship between

the charges and molar absorptivities of the buffer and sample ions. Consequently, it is possible to calculate the detection limits achievable if the molar absorptivity of the absorbing electrolyte is known. A good correlation between calculated and measured detection limits has been found. The detection noise in both separation techniques is a function of the buffer absorption.

In IEC, the buffer concentration has a direct influence on solute retention. The higher the concentration, the earlier the peak elutes and the higher the concentration at the peak maximum becomes. With HPLC detectors, designed for direct UV absorption measurements, the path length is between 5 and 10 mm. Consequently, the UV absorption of the buffers is relatively high, and the limits of the Lambert–Beer law are easily reached. Therefore, it is not possible to measure generally at the absorption maximum of the eluting buffer. The S/N can be optimized for each buffer concentration by variation of the detection wavelength. Usually, a high S/N is obtained close to the cut-off of the eluent.

In CZE, in contrast, a high absorption of the background electrolyte does not lead to a problem, because of the short path length (capillary I.D.). With a standard buffer concentration the absorption does not exceed 0.5 absorption units full-scale. Therefore, it is possible to detect at the absorption maximum of the background electrolyte. The S/N depends strongly on the optical path length in CZE. This is due to the balance between the basic detector noise and the noise caused by the visualizing reagent, which is, on account of the shorter optical path length, different from that in HPLC. The simplified theory by Small and Miller [2] describes only a borderline case for long absorption cells, usually applied in HPLC detectors and with certain values of buffer absorptivity and concentration.

In CZE, despite the short optical path length, relatively low detection limits are achievable. It is no problem to detect ions in the ppb range. One reason for this is that the noise also decreases with the optical path length. The opposite is observed in direct UV detection. Peak dispersion in CZE is usually very low, but not too large concentration differences between the sample and background electrolyte are tolerated.

Indirect UV detection in CZE is a universal and sensitive detection method for solutes without UV absorptivity and permits the detection of inorganic ions in the 0.1 ppm range.

Acknowledgements

We thank Beckman and Millipore (Waters Chromatography Division) for the loan of CZE instruments and Hewlett-Packard for the possibility of working with their instrumentation at Waldbronn. Helpful discussions with P. Jandik (University of Linz, Austria) are greatly appreciated. We thank the Deutsche Forschungsgemeinschaft for financial assistance.

References

[1] M. Denkert, L. Hackzell, G. Schill and E. Sjögren, J. Chromatogr., 218 (1981) 31–43.
[2] H. Small and T. Miller, Anal. Chem., 54 (1982) 463.
[3] P.R. Haddad and P.E. Jackson, Ion Chromatography–Principles and Applications (Journal of Chromatography Library, Vol. 46), Elsevier, Amsterdam, 1990.
[4] J. Weiss, Handbuch der Ionenchromatographie, VCH, New York, 1985.
[5] P. Jandik and W.R. Jones, J. Chromatogr., 546 (1991) 431.
[6] W. Beck and H. Engelhardt, Chromatographia, 33 (1992) 313.
[7] F. Foret, S. Fanali, A. Nardi and P. Bocek, Electrophoresis, 11 (1990) 780.
[8] J. Romano, P. Jandik, W.R. Jones and P.E. Jackson, J. Chromatogr., 546 (1991) 411.
[9] E. Yeung, Acc. Chem. Res, 22 (1989) 125–130.
[10] A. Sokolowskie, T. Fornstedt and D. Westerlund, J. Liq. Chromatogr., 10 (1987) 1629–1662.
[11] T. Fornstedt and D. Westerlund, J. Chromatogr., 648 (1993) 315–324.
[12] S. Hjerten, K. Elenbring, F. Kilar, J. Liao, A.J.C. Chen, C.J. Siebert and M.-D. Zhu, J. Chromatogr., 403 (1987) 47–61.
[13] S. Hjerten, in G. Milleszo (Editor), Topics in Bioelectrochemistry and Bioenergetics, Vol. 2, Wiley, New York, 1978.
[14] W. Beck and H. Engelhardt, Fresenius' J. Anal. Chem., 346 (1993) 618.
[15] M. Ackermans, F.M. Everaerts and J.L. Beckers, J. Chromatogr., 549 (1991) 335–355.
[16] T. Wang and R. Hartwick, J. Chromatogr., 607 (1992) 119–125.

[17] G.J.M. Bruin, A.C. van Asten, X. Xu and H. Poppe, J. Chromatogr., 608 (1992) 97–107.
[18] H. Poppe, J. Chromatogr., 506 (1990) 45–60.
[19] H. Poppe, Anal. Chem., 64 (1992) 1908–1919.
[20] C. Niederländer, F. Steiner and H. Engelhardt, presented at HPLC' 91, Basle, 1991.
[21] D. Bentrop, J. Kohr and H. Engelhardt, Chromatographia, 32 (1991) 171–178.
[22] R.P.W. Scott, Liquid Chromatography Detectors (Journal of Chromatography Library, Vol. 33) Elsevier, Amsterdam, 2nd ed., 1986, p. 23.
[23] H.H. Perkampus, I. Sandeman and C. Timmons, UV-Atlas of Organic Compounds, Vol. V, Butterworths, London, and Verlag Chemie, Weinheim, 1971.